

THERMAL STABILITY OF CELLULOSE NANOCRYSTALS FROM CURAUA FIBER ISOLATED BY ACID HYDROLYSIS

E. CORRADINI, E. A. G. PINEDA,* A. C. CORRÊA,** E. M. TEIXEIRA *** and
L. H. C. MATTOSO **

Department of Materials Engineering, DAEMA/PPGCEM, Federal Technological University of Parana (UTFPR-LD), 80230-901, Londrina, PR, Brazil

**Department of Chemistry, State University of Maringá, 5790, Colombo Av., 87020-900, Maringá, PR, Brazil*

***National Nanotechnology Laboratory for Agriculture, Embrapa/CNPDIA, 13560-970, São Carlos, SP, Brazil*

****Institute of Exact and Earth Sciences, Federal University of Mato Grosso, Campus of Araguaia, Unity I, 78698-000, Pontal do Araguaia, MT, Brazil*

✉ *Corresponding author: E. Corradini, ecorradini@utfpr.edu.br*

Received October 10, 2014

Cellulose nanocrystals were directly extracted from curaua fibers by acid hydrolysis using two different acids (H_2SO_4 and HCl) and a mixture of the two. The morphology of curaua nanocrystals was investigated by atomic force microscopy (AFM) and the effect of the acids on the thermal stability of the cellulose nanocrystals was evaluated by thermogravimetry (TG). Vyazovkin's method was used to determine the apparent activation energy (E_a) of the nanocrystals, which were of similar shape and had a rod-like aspect. The nanocrystals extracted with HCl (NC- HCl) and with the mixture of acids presented higher thermal stability than the nanofiber extracted with H_2SO_4 (NC- H_2SO_4). No directly proportional correlation was found between thermal stability and apparent activation energy (E_a). The average E_a value obtained for NC- H_2SO_4 was similar to that for NC- $\text{H}_2\text{SO}_4/\text{HCl}$, indicating that the presence of sulfate groups influences the degradation behavior, resulting in nanocellulose structures with lower thermal stability, but degradation occurs at higher E_a values.

Keywords: cellulose nanocrystals, curaua fiber, thermal stability, apparent activation energy

INTRODUCTION

Natural fibers, such as sisal, coconut, jute, cotton and curaua, have been studied and commercially used as reinforcement in composites with synthetic and natural polymers.¹ Some recent studies have shown that nanometric cellulose fibers have greater reinforcement potential for polymers than micrometric cellulose fibers. This is due to the higher surface area of cellulose nanocrystals, which promotes stronger interaction with the matrix, thereby improving the mechanical and barrier properties.²⁻⁵

Cellulose nanocrystals can be obtained from several vegetal fibers by acid hydrolysis under controlled conditions (time, temperature and ultrasound treatment).⁶⁻⁸ Hydrolysis is normally performed under sulfuric acid solutions. This process removes the amorphous parts of the

cellulose, leaving well-defined crystals in a stable colloidal suspension.⁹⁻¹⁰ The type of acid used in extraction can affect the thermal stability of cellulose nanocrystals.¹¹⁻¹² Understanding the thermal behavior of these nanocrystals is very important, because several conventional techniques employed in the plastic processing industry are carried out at relatively high temperatures.

In the present work, cellulose nanocrystals were extracted from raw curaua fibers by acid hydrolysis using two different acids separately and mixed ($\text{H}_2\text{SO}_4, \text{HCl}$ and $\text{H}_2\text{SO}_4/\text{HCl}$). The morphology of the curaua nanocrystals was investigated by atomic force microscopy (AFM) and scanning transmission electron microscopy (STEM), their crystallinity by X-ray diffraction (XRD), and the effect of the acids on the thermal

stability of cellulose nanocrystals was evaluated by thermogravimetry (TG).

EXPERIMENTAL

Materials and methods

The curaua fibers were supplied by Embrapa Amazônia Ocidental (Belém, PA, Brazil). Analytical grades of sulfuric (H_2SO_4) and chloridric (HCl) acids (both from Synth) were used. A cellulose membrane (Sigma-Aldrich: D9402) was used to dialyze the nanocrystals.

Preparation of nanocrystals

The curaua fibers were used without any previous treatment. About 5.0 g of fibers were dispersed in 100 mL of 6.5M sulfuric acid at 45 °C and stirred vigorously for 75 min. After that, 500 mL of cold distilled water was added to stop the reaction. The sulfuric acid was partially removed from the resulting suspension by centrifugation at 10,000 rpm for 10 minutes. The non-reactive sulfate groups were removed by centrifugation, followed by dialysis. The fibers were then resuspended and dialyzed with tap water through a cellulose membrane, until the pH reached 6 to 7. The resulting suspension was ultrasonicated for 5 min and stored in a refrigerator after the addition of a few drops of chloroform. The same procedure was used to extract nanocrystals, using HCl (1 M) and H_2SO_4 (6.5M):HCl(1M) (1:1; v/v). Parts of the neutral suspensions were freeze-dried.

Morphological characterization of curaua nanocrystals: Atomic force microscopy (AFM)

The AFM measurements were taken in a Dimension V (Veeco) atomic force microscope. The images were obtained in tapping mode at a scan rate of 1 Hz, using Si tips with a radius of curvature of 11 ± 3 nm and a slope angle of about 10 °, attached to a cantilever (T-shape) with a spring constant of 42 ± 5 N m^{-1} . A drop of diluted aqueous suspension of nanocrystals was placed on an optical glass slide, allowed to dry at room temperature for 12 h, and then analyzed by AFM.

Scanning transmission electron microscopy (STEM)

Nanofiber samples for analysis were examined using a TecnaiG2 F20 SEM operating in transmission mode (STEM). A droplet of diluted suspension was deposited on a carbon microgrid (400 mesh) and allowed to dry. The grid was stained with a solution of 1.5% uranyl acetate and dried at room temperature.

X-ray diffraction (XRD)

Diffraction patterns were recorded using a Rigaku diffractometer operating at 50 kV, 100 mA and $CuK\alpha$ radiation ($k = 1540 \text{ \AA}$). The samples were scanned in the 2θ range, varying from 5 to 40° (2° min^{-1}). The crystallinity index (I_c) was calculated from the height

of the 200 peak (I_{200} , $2\theta = 22.6^\circ$) and the minimum intensity between the 200 and 110 peaks (I_{am} , $2\theta = 18^\circ$), as described by Buschle-Diller-Zeronian:¹³

$$I_c = \left(\frac{1 - I_{am}}{I_{200}} \right) \times 100 \quad (1)$$

Thermogravimetry analysis (TG)

The fibers and nanocrystals were analyzed by thermogravimetry (TG) and derivative thermogravimetry (DTG), using a TA Q500 thermogravimetric analyzer (TA Instruments, New Castle, DE, USA). The TG/DTG curves of the curaua fibers and nanocrystals were measured in air and nitrogen atmospheres at 10 °C/min. The experiments for the kinetic study were carried out in nitrogen atmosphere at 5, 10, 15 and 20 °C/min. All the measurements were taken at a flow rate of 60 mL/min, in a platinum crucible, using a sample mass of about 5 mg.

The TG/DTG curves obtained at 5, 10, 15 and 20 °C min^{-1} in nitrogen atmosphere were analyzed by Vyazovkin's method¹⁴ (Eq. 2) to determine the apparent activation energy (E_a), which was calculated as a function of the degree of reaction:

$$\frac{\ln \beta}{T^2} = \ln \left[\frac{RA}{Eg(\alpha)} \right] - \frac{E}{RT} \quad (2)$$

where α is the conversion fraction, $g(\alpha)$ is the integral reaction model, β is the heating rate, T is the absolute temperature, A is the pre-exponential factor, E is the activation energy, and R is the gas constant.

RESULTS AND DISCUSSION

Figure 1 shows the AFM image of curaua nanofiber extracted using H_2SO_4 solution. All the nanocrystals had a similar shape and a rod-like aspect. The average diameter (D) was about 30 nm and the length (L) was a few nanometers. However, these values, particularly the diameter, may be overestimated due to the AFM tip-broadening effect during scanning.¹² Figure 2 shows the individual nanocrystals observed by STEM, while Table 1 lists their real values of average diameter and length. These dimensions were calculated for about 60 nanocrystals, using ImageJ software. No significant differences in diameter and length were detected among the different acid-treated nanocrystals. The suspensions of the resulting nanocrystals two months after extraction are also shown in Fig.2. The stability of the suspensions clearly decreased when HCl acid was used for extraction. The suspension obtained from the mixture of acids exhibited an intermediate behavior between the suspensions resulting from each individual acid. Chloride ions are easily removed by repeated washing in water. The electrostatic force is not

enough to cause repulsion between particles, and therefore they agglomerate.¹¹⁻¹² Using a mixture of H_2SO_4/HCl acids in the acid hydrolysis to obtain nanocrystals, the resulting suspensions are expected to be more dispersed than those obtained when using only HCl . This was an indication that some superficial charge was introduced on the cellulose surface in this acid condition. The H_2SO_4 -treated sample showed sulfate groups on the nanofiber surface, generating a charge that stabilized the suspension due to the repulsion between them.

Figure 3 shows the XRD patterns of raw curaua and its nanocrystals. These diffractograms display a well-defined main peak at around $2\theta = 22.6^\circ$, which is characteristic of type I cellulose.

In this figure, note that the acid treatments caused a slight narrowing of the peak for the nanocrystals, which, as expected, resulted in more crystalline structures than those of the raw fiber, as indicated in Table 1 (I_c values). These crystallinity values were also quite similar and independent of the acid treatment.

Each of the three components of vegetal fibers (lignin, cellulose and hemicellulose) has its own thermal behavior, which depends on the chemical composition, microstructure and three-dimensional nature of fiber. These components behave differently if they are isolated or if they are combined within each single cell of the fiber structure.¹⁵

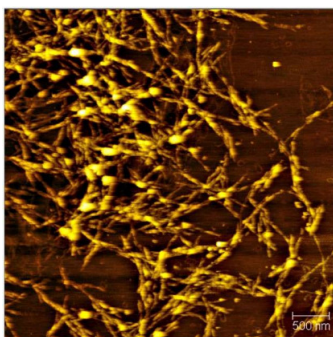


Figure 1: AFM image of curaua nanocrystals obtained using H_2SO_4 acid

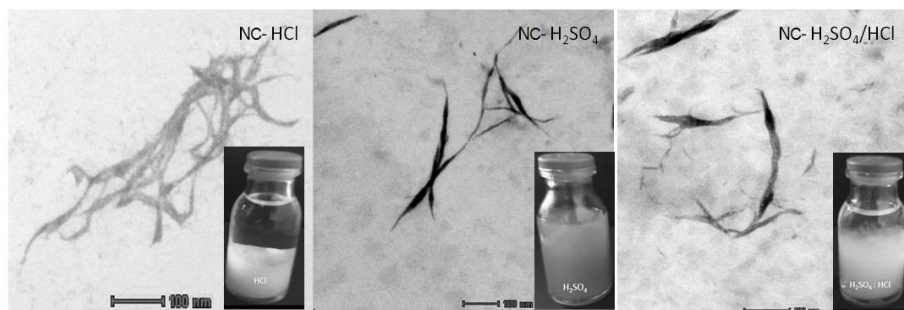


Figure 2: Transmission electron micrographs (scale 100 nm) and physical aspect of curaua nanocrystal suspensions (after 2 months) extracted under different acid conditions as indicated in the figure

Table 1
Dimensions of nanofibers and crystallinity index for the samples

Sample	Diameter (nm)	Length (nm)	I_c (%)
Raw curaua	--	--	72.6
NC-HCl	7 ± 2	83 ± 24	80.6
NC- H_2SO_4	6 ± 1	78 ± 31	78.8
NC- H_2SO_4/HCl	6 ± 1	91 ± 29	79.0

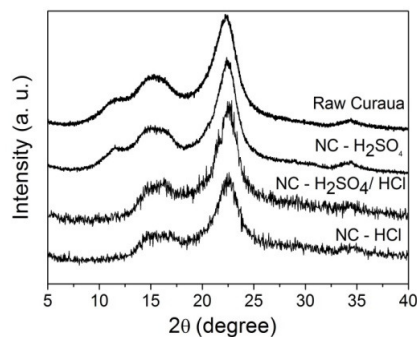


Figure 3: X-ray diffraction patterns of raw curaua fiber nanocrystals

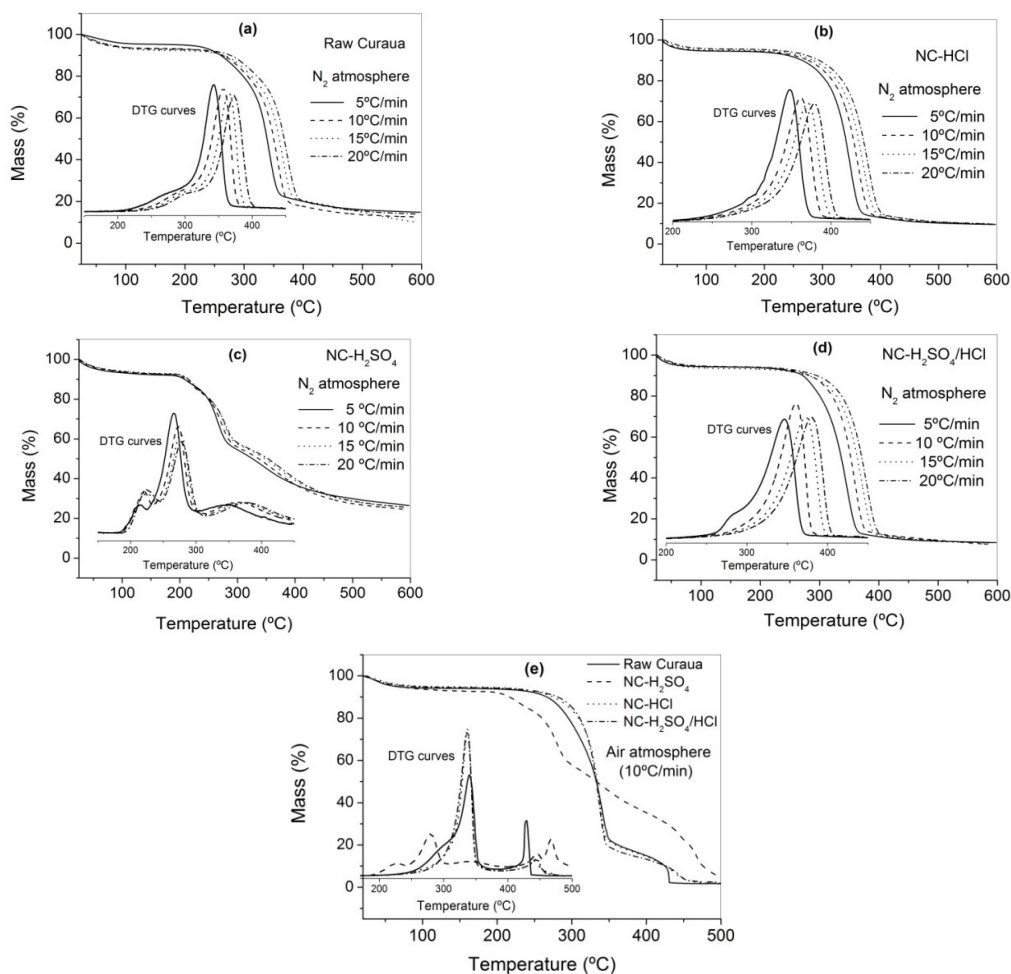


Figure 4: TG/DTG curves at 5, 10, 15 and 20 °C min⁻¹ in nitrogen for raw (a), n-HCl (b), NC-H₂SO₄ (c) and NC-H₂SO₄/HCl (d) acid treated curaua fiber; curves at 10 °C min⁻¹ in air atmosphere for raw curaua fibers and nanocrystals (e)

The thermal degradation of lignocellulosic components occurs in several successive steps within a temperature range of 220 °C to 550 °C. Hemicellulose degrades at about 240-310 °C,

whereas cellulose degrades between 310 °C and 360 °C and lignin has been shown to degrade in wide temperature intervals (220-550 °C).¹⁶⁻¹⁸

Figure 4 shows TG/DTG curves in nitrogen and air atmospheres for the curaua fibers and nanocrystals. A shift to higher temperatures is observed in the TG/DTG curves obtained in nitrogen atmosphere when compared with the curves obtained in air atmosphere. This occurs because oxygen generally tends to act as an oxidizing agent, which increases the speed of thermal degradation reactions.¹⁶

In both atmospheres, the DTG curves obtained for curaua fiber showed two consecutive thermal events. The first, a shoulder, is attributed to hemicellulose degradation. The second event is a well-defined peak attributed to cellulose depolymerisation.¹⁶ A third event is observed only in air atmosphere, which is attributed to the oxidation of partially decomposed components.¹⁸ The TG/DTG curves obtained for nanocrystals extracted with hydrochloric acid and the mixture of hydrochloric and sulfuric acid exhibited a similar profile in both atmospheres. This indicates that these nanocrystals have similar chemical compositions and structures. However, the TG/DTG curves obtained for nanocrystals treated with sulfuric acid revealed differences in thermal behavior in comparison to that of the other nanocrystals, probably due to the presence of

sulfate groups, which promote dehydration reactions that release water and which can influence cellulose degradation reactions.¹³

Table 2 describes the parameters that were determined based on the TG and DTG curves: weight loss from 25 to 120 °C, initial temperature of degradation (T_{onset}), weight loss due to thermal degradation and mass residue at 450 °C.

Note that the weight loss resulting from water loss between 25 and 120 °C varied little among the samples. A comparison of the T_{onset} values of curaua fiber and those obtained for nanocrystals indicated that the T_{onset} values of nanocrystals extracted with HCl and with the mixture of acids were higher than those of the curaua fibers. This increase in the thermal stability of nanocrystals was due to the extraction of hemicellulose and lignin, which degrade at lower temperatures than cellulose. However, the nanocrystals extracted with sulfuric acid showed lower T_{onset} values than the other nanocrystals and the raw fiber. This may be due to the presence of sulfate groups introduced during the hydrolysis process on the surface of cellulose, which catalyze thermo-oxidative degradation, considerably decreasing its thermal stability.⁹⁻¹¹

Table 2

Parameters determined from thermogravimetric curves (TG) and their respective derivatives (DTG) of raw curaua fiber and nanocrystals: water uptake from 25-120°C, T_{onset} (temperature onset), mass loss (%) resulting from thermal degradation and residue content at 600°C

Fiber	Atmosphere	Water uptake 25-120 °C (%, mass)	T_{onset} (°C)	Mass loss (%)	Residue at 450 °C
Raw curaua	5 °C/min (N ₂)	4.6	237	72	14
	10 °C/min (N ₂)	6.6	266	72	17
	10 °C/min (air)	6.3	256	90	17
	15 °C/min (N ₂)	7.3	269	69	17
	20 °C/min (N ₂)	6.7	272	72	17
NC- HCl	5 °C/min (N ₂)	5.4	267	77	11
	10 °C/min (N ₂)	6.7	268	78	11
	10 °C/min (air)	5.3	272	92	4
	15 °C/min (N ₂)	5.0	282	77	11
	20 °C/min (N ₂)	4.3	293	78	11
NC- H ₂ SO ₄	5 °C/min (N ₂)	7.2	198	62	31
	10 °C/min (N ₂)	6.7	201	65	31
	10 °C/min (air)	5.4	206	89	23
	15 °C/min (N ₂)	6.3	206	63	31
	20 °C/min (N ₂)	6.6	209	63	31
NC- H ₂ SO ₄ / HCl	5 °C/min (N ₂)	5.7	261	79	10
	10 °C/min (N ₂)	5.6	292	76	9
	10 °C/min (air)	5.5	285	88	4
	15 °C/min (N ₂)	6.4	304	75	10
	20 °C/min (N ₂)	5.4	299	76	10

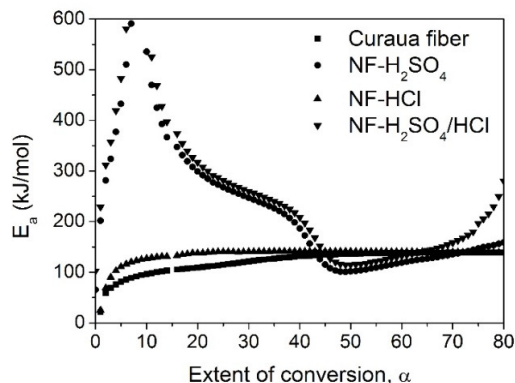


Figure 5: Apparent activation energy as a function of conversion for raw curaua fiber and nanocrystals (N_2 atmosphere)

The DTG curves of nanofiber extracted with H_2SO_4 showed three peaks. The first peak at around $220\text{ }^\circ\text{C}$ is attributed to the degradation reaction of cellulose chain units containing sulfate groups, because they promote the dehydration reactions that release water and catalyze cellulose degradation reactions. The second and third peaks are attributed to the degradation reactions of cellulose chains with lower contents of sulfate groups and/or chains that were not in contact with the sulfuric acid.¹¹⁻¹²

The residue remaining after the thermal degradation, which took place at $450\text{ }^\circ\text{C}$ in both atmospheres, is inorganic ash, which is naturally present as a constituent of fibers. The residue content of the nanofiber extracted with sulfuric acid was higher than that of the other fibers. Roman and Winter¹¹ showed that the amount of charred residue at $350\text{ }^\circ\text{C}$ in air atmosphere was larger in cellulose crystals with a larger number of sulfate groups. Therefore, the amount of charred residue determined in TG curves is directly proportional to the amount of sulfate groups in nanocrystals obtained by hydrolysis acid.

Figure 5 illustrates the apparent activation energy (E_a) as a function of the degree of conversion (α). For raw curaua, the values of E_a increased slightly in response to the increase in α from 0.0 to 0.40, remaining approximately constant for higher values of α . The E_a values for the NC-HCl were approximately constant in the entire interval of conversion and were similar to that of raw fiber. The value of E_a as a function of α varied significantly between then a nocrystals extracted using H_2SO_4 acid (NC- H_2SO_4 and NC- H_2SO_4/HCl), which showed similar profiles. This variation confirmed the complexity of the decomposition behavior and the existence of

multiple decomposition steps due to the incorporation of sulfate groups. The E_a values obtained for NC- H_2SO_4 and NC- H_2SO_4/HCl were higher than those obtained for raw curaua and NC-HCl for α was between 0.02 and 0.4. In the conversion interval of 0.4 to 0.7, the E_a values were lower than those obtained for other fibers. This stage of the thermal degradation was probably catalyzed by sulfate groups, thus decreasing the E_a values, as reported in the literature.^{11,20} At a higher degree of conversion, the E_a values increased due to the presence of residual char, which slows down the degradation reaction. The average activation energies in the overall process were 123 kJmol^{-1} , 130 kJmol^{-1} , 223 kJmol^{-1} and 264 kJmol^{-1} for curaua fiber, NC-HCl, NC- H_2SO_4 and NC- H_2SO_4/HCl , respectively. The mean E_a values fall within the same range as that reported for bacterial cellulose nanofiber.¹¹ No directly proportional correlation with thermal stability was found. These results point to the need for further mechanistic studies about cellulose nanofiber degradation, particularly the influence of the incorporation of sulfate groups on this mechanism.

CONCLUSION

Curaua nanocrystals were obtained by means of different acid treatments (extracted with HCl, H_2SO_4 and with a mixture of these acids). These nanocrystals showed no morphological differences, and all of them presented a rod-like aspect with a diameter and length of about 6 nm and 100 nm, respectively. The nanocrystals also showed similar crystallinity, which did not influence their thermal degradation behavior. The nanocrystals extracted with HCl (NC-HCl) and with the mixture of acids presented higher thermal

stability than the nanocrystals extracted with H₂SO₄ (NC-H₂SO₄). There was no directly proportional correlation between thermal stability and apparent activation energy (E_a). The mean E_a value obtained for NC-H₂SO₄ was similar to that of NC-H₂SO₄/HCl, indicating that these samples presented a complex thermal degradation mechanism, which can probably be attributed to the heterogeneous incorporation of sulfate groups in the cellulose structure.

ACKNOWLEDGEMENTS: The authors gratefully acknowledge Embrapa Amazonia Pantanal for donating the curaua fiber samples, and the Brazilian research funding agencies CNPq (National Council for Scientific and Technological Development) and FAPESP (São Paulo Research Foundation) for their financial support of this work.

REFERENCES

- ¹ C. J. Chirayil, L. Mathew and S. Thomas, *Rev. Adv. Mater. Sci.*, **37**, 20 (2014).
- ² S. J. Eichhorn, A. Dufresne, M. Aranguren, N. E. Marcovich, J. R. Capadona *et al.*, *J. Mater. Sci.*, **45**, 1 (2009).
- ³ Y. Habibi, L. Lucia and O. J. Rojas, *Chem. Rev.*, **110**, 3479 (2010).
- ⁴ A. Campos, A. C. Correa, D. Cannella, E. M. Teixeira, J. M. Marconcini *et al.*, *Cellulose*, **20**, 1491 (2013).
- ⁵ F. Bettaieb, R. Khiari, A. Dufresne, M. F. Mhenni and M. N. Belgacem, *Carbohydr. Polym.*, **123**, 99 (2015).
- ⁶ O. Faruk, A. K. Bledzki, H.-P. Fink and M. Sain, *Mater. Sci. Eng.*, **299**, 9 (2014).
- ⁷ M. A. Henrique, W. P. Flauzino Neto, H. A. Silvério, D. F. Martins, L. V. A. Gurgel *et al.*, *Ind. Crop. Prod.*, **76**, 128 (2015).
- ⁸ L. A. de S. Costa, A. F. Fonseca, F. V. Pereira and J. Druzian, *Cellulose Chem. Technol.*, **49**, 127 (2015).
- ⁹ M. M. S. Lima and R. Borsali, *Macromol. Rapid Comm.*, **25**, 771 (2004).
- ¹⁰ A. Dufresne, *J. Nanosci. Nanotechnol.*, **6**, 322 (2006).
- ¹¹ M. Roman and W.T. Winter, *Biomacromolecules*, **51**, 671 (2004).
- ¹² B. Wang and M. Sain, *BioResources*, **2-3**, 371(2007).
- ¹³ G. Buschle - Diller and S. H. Zeronian, *J. Appl. Polym. Sci.*, **45**, 967 (1992).
- ¹⁴ S. Vyazovkin and C. A. Wight, *Ann. Rev. Phys. Chem.*, **48**, 125 (1997).
- ¹⁵ I. Kvien, B. S. Tanem and K. Oksman, *Biomacromolecules*, **6**, 3160 (2005).
- ¹⁶ T. P. Sathishkumar, P. Navaneethakrishnan, S. Shankar, R. Rajasekar and N. Rajini, *J. Reinf. Plast. Comp.*, **32**, 1457 (2013).
- ¹⁷ V. Alvarez and A. Vázquez, *Polym. Degrad. Stabil.*, **84**, 13 (2004).
- ¹⁸ V. Alvarez, E. Rodrigues and A. T. Vázquez, *J. Therm. Anal. Calorim.*, **85**, 383 (2006).
- ¹⁹ W. Li, Y. M. Wing and L. Ye, *Compos. Sci. Technol.*, **60**, 2037 (2000).
- P. Aggarwal, D. Dollimore and K. Heon, *J. Therm. Anal.*, **50**, 7 (1997).